Ab initio study of the two lowest triplet potential energy surfaces involved in the N(^4S)+NO ($X\ ^2\Pi$) reaction

P. Gamallo, Miguel González,[a)] and R. Sayós[b)]
*Departament de Química Física i Centre de Recerca en Química Teòrica, Universitat de Barcelona,
C / Martí i Franquès 1, 08028 Barcelona, Spain*

This work presents *ab initio* electronic structure calculations of the two possible N(^4S) +NO($X\ ^2\Pi$) abstraction reaction channels on the lowest $^3A''$ and $^3A'$ potential energy surfaces (PESs). Complete active space self-consistent-field (CASSCF) calculations, second-order perturbation calculations (CASPT2), and multireference configuration interaction calculations (MR-CI) based on CASSCF wave functions, along with some coupled cluster (CC) calculations were carried out by using the standard correlation-consistent (cc-pVnZ and aug-cc-pVnZ, n=D,T,Q,5) Dunning's basis sets. It was shown that there was no energy barrier along the minimum energy path in the $^3A''$ PES for the *N*-abstraction reaction channel. However, an energy barrier (6.74 kcal/mol) was located in the $^3A'$ PES. This energy barrier was considerably smaller than the previously reported MR-CCI value (14.4 kcal/mol). It was established that the N and O 2s electron correlation, neglected in previous studies of these authors, was the main source of this energy decrease. As a result, the present *ab initio* data will produce larger values of the thermal rate constants at high temperatures. High-energy barriers were found for the O-abstraction reaction channel in both PESs (41.13 and 30.77 kcal/mol for $^3A''$ and $^3A'$, respectively), which agree with the accepted idea that this channel will be only important at high collision energies. Nonetheless, current *ab initio* results show that this channel will be open at not very high collision energies (e.g., over 30 kcal/mol could take place). Experimental studies on the O-abstraction reaction channel are missing and would be useful to confirm its *ab initio* expected importance. © *2003 American Institute of Physics.* [DOI: 10.1063/1.1574315]

I. INTRODUCTION

The elementary gas-phase reaction of N(^4S) with nitric oxide,

$$N(^4S) + NO(X\ ^2\Pi) \rightarrow O(^3P) + N_2(X\ ^1\Sigma_g^+)$$
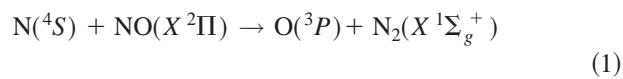
$$\Delta_r H_{0K}^o = -75.01 \text{ kcal/mol (Ref. 1)}, \tag{1}$$

and its reverse reaction play an important role in atmospheric chemistry. The direct reaction is thought to be a dominant step for odd nitrogen removal in the upper stratosphere, the mesosphere and the thermosphere of the Earth, and possibly also in Mars and Venus.[2–4] The accuracy of the rate constants for this reaction over a wide range of temperatures [e.g., from 185 K in mesopause to approximately 1000 K at 250 km altitude (upper thermosphere)[5]] is of great importance for the modeled concentration of NO$_x$ species in these atmospheric regions for varying levels of solar activity. On the other hand, this reaction has been also proposed as one important step to remove the NO molecules produced in heterogeneous catalytic processes (e.g., in SiO$_2$-based materials) for airflow cases; this NO production could have great

effects for the heat flux on the thermal protection systems used in atmospheric reentry vehicles (e.g., space shuttle, OREX, . . .).[6]

In spite of this reaction having been extensively studied from an experimental point of view, particularly for the room temperature rate constant[3] ($1.7\times10^{-11} \leqslant k_{298\ K} \leqslant 4.5 \times10^{-11}$ cm^3 molecule^{-1} s^{-1}), there are still some doubts about its slight temperature dependence. Thus, several laboratory studies covering different temperature ranges have shown somewhat different expressions. Baulch *et al.*[7] presented a recommended value at high temperatures equal to $7.1\times10^{-11}e^{-790/T}$ cm^3 molecule^{-1} s^{-1} between 1400–4000 K. The Jet Propulsion Laboratory[8] proposed $2.1\times10^{-11}e^{(100\pm100)/T}$ cm^3 molecule^{-1} s^{-1} based in published kinetic data within the interval 200–400 K. Other studies based in terrestrial or martian atmospheric NO modeling have derived either a negative temperature dependence (e.g., $1.6\times10^{-10}e^{-460/T}$ cm^3 molecule^{-1} s^{-1} for $T>300$ K (Ref. 2) and $2.5\times10^{-10}(T/300)^{1/2}e^{-600/T}$ cm^3 molecule^{-1} s^{-1} between 100–200 K (Refs. 9 and 10) or a positive one [e.g., $2.2\times10^{-11}e^{160/T}$ cm^3 molecule^{-1} s^{-1} for $213 \leqslant T \leqslant 369$ K (Ref. 3)]. Besides kinetic studies, there are only very few experimental studies dealing with the dynamics properties of this reaction. Thus, only earlier studies measured some information on the product N$_2$ vibrational distributions, indicating a product vibrational energy fraction of 0.25–0.28.[11,12] How-

[a)]Electronic mail: miguel@qf.ub.es
[b)]Authors to whom correspondence should be addressed. Electronic mail:
r.sayos@qf.ub.es, miguel@qf.ub.es

ever, another study indicated a higher fraction due to the $75 \pm 5\%$ of the N_2 molecules appeared with $v' > 4$.[13]

In several preceding papers we presented different theoretical approaches for this reaction and we also gave a detailed review of the main experimental and theoretical data that had been published for this reaction. We constructed an analytical potential energy surface (PES) (Ref. 14) based on limited *ab initio* information[15] for the ground $^3A''$ PES, and we carried out dynamics studies by means of the quasiclassical trajectory (QCT) method,[16] reduced quantum approaches[17] (reactive-infinite-order sudden approximation) or simple models[18] (angle-dependent line-of-centers model). Lately, QCT calculations on a new $^3A''$ PES,[19] which was fitted using the same *ab initio* data [15] but adding new interpolated semiempirical points, reported good thermal rate constants for $200 \leq T \leq 1000$ K, with the inclusion of the reactant statistical degeneracy factor (i.e., 3/16), missing in previous works. The same authors presented a QCT study[20] on this reaction taking also into account the first excited PES ($^3A'$), previously fitted for the reverse reaction by other authors.[21] It was concluded that only at high energies (i.e., 1–3 eV) the excited PES became important.

For the second reaction channel (i.e., the O-abstraction process):

$$N(^4S) + N'O\,(X\,^2\Pi) \rightarrow N'(^4S) + NO\,(X\,^2\Pi)$$

$$ \tag{2}$$
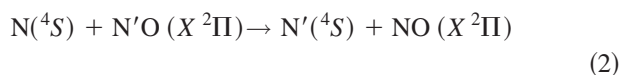
$$\Delta_r H^0_{0\,K} = 0 \;\; \text{kcal/mol},$$

there is almost no information. Only some experiments[22,23] at very high energies with ^{13}N and pure NO indicated that channel 2 yielding ^{13}NO could account for up to a 20% of the total reaction, although with the possible contribution of the first excited states of nitrogen [i.e., $N(^2D, ^2P)$].

The present work presents a new accurate *ab initio* molecular electronic structure study of the $N(^4S) + NO$ reaction taking into account both PESs (i.e., $^3A''$ and $^3A'$), and also the two possible reaction channels. Previous theoretical studies proposed that more extensive and accurate *ab initio* characterization of $^3A'$ and $^3A''$ PESs was necessary to construct reliable analytical PESs valid for dynamics and kinetics studies, as it is our goal here. New analytical PESs based in grids of *ab initio* points are at present practically finished and QCT and wave packet studies on this reaction are also in progress.

Section II will offer a summary of the *ab initio* methodology applied in this work. Section III will provide the *ab initio* results on the stationary points of both PESs ($^3A''$ and $^3A'$), and the corresponding minimum energy reaction paths (MEPs) connecting minima (MIN), and transition states (TS). Finally, Sec. IV will summarize the main concluding remarks.

II. THEORETICAL METHODS

A similar strategy as that used in our recent study of the $N(^4S) + O_2$ reaction[24] was also applied in the present work. Thus, *ab initio* calculations have been carried out with the MOLCAS 4.1 (Ref. 25) package of programs. The complete active space self-consistent field method (CASSCF) (Refs. 26, 27) was employed throughout this study, always choosing the lowest root in C_s symmetry for both triplet PESs (i.e., $^3A''$ and $^3A'$). These two PESs are the unique ones that correlate reactants and products for reaction (1). The other PESs that also arise in reactants (i.e., $^5A''$ and $^5A'$), only correlate with very excited products [i.e., $O(^3P) + N_2$ $(A\,^3\Sigma_u^+)$]. The location of the different stationary points on the PESs was achieved by optimization searches of both minima and transition states employing analytical CASSCF gradients. Full characterization of them was performed by calculating the numerical Hessian matrix at the optimized geometries. Calculations at second-order perturbation theory based on a zeroth-order CASSCF wave function (CASPT2 method) using the standard correction (i.e., std) or some of the more accurate G_i ($i=1,2,3$) variants[28] as implemented in MOLCAS 4.1 were applied to improve the stationary points obtained at the CASSCF level. In some cases, a grid of CASPT2 points was generated to search directly for the stationary point. Thus, local fits were performed by means of bicubic splines[29] or Taylor expansions in the bond angle together with symmetry adapted internal coordinate expansion in the bond lengths to obtain the optimal geometry and the harmonic frequencies at the CASPT2 level by using the SURVIBTM code of molecular rovibrational analysis.[30]

In the present study all the molecular orbitals (MO) arising from the 1s atomic orbitals were kept frozen, and two active spaces for the NNO system were considered: (a) the full-valence active space with all the atomic 2s and 2p electrons distributed among the corresponding derived bonding and antibonding MOs [i.e., CAS (16,12)], and (b) a smaller active space with only the atomic 2p electrons [i.e., CAS (10,9)], taking the 2s-derived MOs as inactive. This latter active space has been assumed to be accurate enough for this system in the most extensive preceding *ab initio* paper on this reaction.[15] Natural MO occupation was checked for all stationary points. The CAS (16,12) comprising 16 electrons in 12 orbitals (9 a' and 3 a'') generates 56 664 and 56 592 configuration state functions (CSFs) for the $^3A''$ and $^3A'$ PESs, respectively, while the CAS(10,9) with 10 electrons in 9 orbitals (6 a' and 3 a') only 3804 and 3756, respectively. The major part of CASSCF and CASPT2 calculations used the lower active space [i.e., CAS(10,9)] as it reduced a lot the computer time but the accuracy was suitable in comparison with available experimental data and when comparing with CAS (16,12) results. The N and O 1s and 2s MOs were optimized at the CASSCF level; in some CASPT2 calculations, the derived 1s and 2s MOs were kept frozen to compare with earlier CASSCF followed by multireference contracted CI (MR-CCI) calculations.[15] The present results will show the importance of the 2s dynamical correlation energy in the characterization of this reaction on both surfaces, not considered in previous studies.[15] Moreover, two additional *ab initio* methods were also used to check the accuracy in the correlation energies calculated: (a) uncontracted multireference singles and doubles configuration interactions including

Davidson correction for quadruple excitations (i.e., MR-CI+Q),[31] using the CASSCF(10,9) MOs and all the CSFs with a weight up to 0.0005 in the CASSCF wave function, and (b) coupled cluster method with perturbative contribution at triple excitations[32] [i.e., CCSD(T)] using the MOs derived from a restricted open shell Hartree–Fock calculation.

The standard correlation-consistent (cc-pVnZ and aug-cc-pVnZ, n=D,T,Q,5) Dunning's basis sets[33] were used in the present study. Supermolecule calculations were considered too in the determination of the energies of the stationary points within each PES.

III. RESULTS AND DISCUSSION

A. Stable species and reaction exoergicity

Table I summarizes the calculated bond length, the harmonic vibrational frequency, and the dissociation energy of both diatomic molecules along with the reaction exoergicity (1) for different *ab initio* levels. The CASSCF calculations with larger basis sets and both active spaces show that the lower active space is accurate enough for describing these properties. However, the introduction of dynamical correlation energy by means of the CASPT2 method is necessary to obtain results in close agreement with experimental data. The comparison of the CASSCF geometries with the experimental data shows a small but rather clear effect of the size of the basis set on the optimal bond lengths and harmonic frequencies, which slowly tend to the experimental ones. Nevertheless, the description of both N_2 and NO dissociation energies is a bit worse. The CASPT2 calculations by using the G_i variants give similar results although much better than the CASPT2 with the standard (std.) Fock matrix, as it should be expected.[28] The N_2 and NO dissociation energies show a significant error (errors of approximately -4.5% with respect to the experimental values) even with the inclusion of the geometry optimization at the same level [i.e., CASPT2 G2(10,9)/cc-pVTZ], which causes a similar error in exoergicity. Nevertheless, the results are very good with the largest basis set and active space [i.e., CASPT2 G2(16,12)/cc-pVQZ gives errors lower than -1.2%]. The CCSD(T) and MR-CI+Q energies present as well good results, which improve with the size of the basis set and are quite close to the CASPT2 (10,9) G2 energies. Present MR-CI+Q results are quite good in spite of the N and O $2s$ electrons are not correlated, such as was also observed in similar MR-CCI+Q calculations.[15] The difficulty in the theoretical treatment in diatomic molecules is well known and can only be amended with very refined and computationally expensive *ab initio* calculations with inclusion of large primitive basis sets[35] or by using also complete basis set (CBS) limits.[36,37] However, as the main purpose of the present study is to characterize all the stationary points of the two lowest triplet PESs involved in the title reaction by using the same *ab initio* level, the CASPT2 G2(10,9)/cc-pVTZ level accuracy can be suitable for a later construction of the $^3A''$ and $^3A'$ analytical PESs, where usually some experimental diatomic data are often introduced.

B. Characterization of the lowest $^3A''$ potential energy surface

The *ab initio* study of the MEP on the $^3A''$ PES for reaction channel (1) shows only one transition state. Table II gives its properties for different *ab initio* calculations. The CASSCF method reports an earlier transition state (i.e., long NN distance) for both active spaces with several basis sets. The corresponding geometry and harmonic vibrational frequencies are very close to the preceding CASSCF results[15] with a Duijneveldt basis set. The small energy barrier clearly disappears as the dynamical correlation energy is introduced by means of the CASPT2 method. This fact is in agreement with previous multireference contracted CI results,[15] where it was observed a very small energy barrier of 0.5 kcal/mol. Nevertheless, the same authors recognized that due to the limitations of their calculations probably no additional barrier should be expected. To make sure that there was no energy barrier at longer NN distances, as it was observed when dynamical correlation energy was introduced,[15] not only CASPT2 energies at the CASSCF geometries were calculated but also an extensive grid of CASPT2 (10,9) G2 /cc-pVTZ energies along the MEP (approx. 180 points). The local fit of these points[30] showed an energy profile without any energy barrier from reactants to products.

The CCSD(T) and the uncontracted MR-CI+Q calculations at the CASSCF(10,9) optimal geometries seem to confirm also the absence of any energy barrier. Present MR-CI calculations used the following nine reference CSFs, where the electronic occupation of the $6a'$ and $3a''$ MOs are indicated: (222100 210), (220120 210), (221110 210), (222100 012), (122101 111), (212110 111), (022102 210), (112111 210), and (221110 201) with a total weight of 0.9837. This originated the following number of CSFs depending on the basis set: 318644 (cc-pVDZ), 2202524 (cc-pVTZ), 1177190 (aug-cc-pVDZ), and 5778909 (aug-cc-pVTZ) to be compared with previous MR-CCI calculations[15] with approximately 1000000 of CSFs. Our MR-CI calculations kept frozen also the N and O $2s$ electrons to compare directly with previous studies.[15] The importance of the N and O $2s$ electron correlation, which was neglected in the past, is here ascertained by means of the CASPT2 method. Thus, for example, the CASPT2(10,9) G2 energy for cc-pVDZ, cc-pVTZ, and cc-pVQZ basis sets at the corresponding CASSCF optimal geometry (-1.90, -4.88, and -6.12 kcal/mol, respectively; see Table II) become more positive when $2s$ electron correlation is neglected (i.e., -0.58, -3.14, and -4.07 kcal/mol, respectively). This energy lowering probably would vanish the MR-CCI energy barrier[15] or our MR-CI calculations at its optimal geometry (possibly with a longer NN distance than in the CASSCF level). A similar trend with the addition of the N and O $2s$ electron correlation has also been revealed in our similar study[24] on the two lowest PESs (i.e., $^2A'$ and $^4A'$) of the N(^4S) +O_2 reaction.

The second reaction channel (2) have been also studied by using the CASSCF(10,9) and the CASPT2 (10,9) G2 methods and the cc-pVTZ basis set. This *ab initio* level seems accurate enough to describe this less important channel, as it has been shown too in the reaction channel (1) study or in other similar recent studies for the N(^4S) + O_2

J. Chem. Phys., Vol. 118, No. 23, 15 June 2003

N+NO reaction   10605

TABLE I. *Ab initio* properties of reactants and products.[a]

Method	Basis set	$N(^4S)+NO$				$O(^3P)+N_2$				$\Delta D_e{}^{\text{b}}$
		E/a.u.	R_e/Å	ω_e/cm^{-1}	D_e/kcal mol^{-1}	E/a.u.	R_e/Å	ω_e/cm^{-1}	D_e/kcal mol^{-1}	kcal mol^{-1}
CASSCF(16,12)	cc-pVDZ	−183.763 88	1.1640	1914.45	125.21	−183.891 32	1.1161	2360.34	205.17	−79.97
	cc-pVTZ	−183.807 10	1.1587	1895.64	129.73	−183.937 55	1.1056	2345.80	211.58	−81.86
	cc-pVQZ	−183.819 42	1.1570	1895.71	130.66	−183.950 53	1.1039	2345.34	212.93	−82.27
	aug-cc-pVDZ	−183.773 34	1.1657	1894.87	127.15	−183.900 76	1.1170	2344.82	207.11	−79.95
	aug-cc-pVTZ	−183.808 75	1.1586	1888.78	129.90	−183.939 80	1.1054	2343.00	212.14	−82.23
CASPT2(16,12) std	cc-pVDZ	−184.036 28			139.52	−184.128 06			198.36	−58.84
	cc-pVTZ	−184.206 80			141.23	−184.317 59			210.74	−69.52
	cc-pVQZ	−184.257 16			145.29	−184.369 76			215.95	−70.65
	aug-cc-pVDZ	−184.088 01			133.26	−184.192 53			198.84	−65.58
	aug-cc-pVTZ	−184.218 28			146.18	−184.329 03			211.58	−69.50
CASPT2(16,12) G2	cc-pVDZ	−184.030 28			146.94	−184.123 79			205.62	−58.68
	cc-pVTZ	−184.196 91			147.29	−184.312 56			219.86	−72.57
	cc-pVQZ	−184.246 56			151.81	−184.364 36			225.73	−73.92
	aug-cc-pVDZ	−184.078 59			139.18	−184.187 64			207.61	−68.43
	aug-cc-pVTZ	−184.207 65			148.60	−184.323 68			221.41	−72.81
CASSCF(10,9)	cc-pVDZ	−183.754 79	1.1619	1926.77	119.52	−183.878 32	1.1144	2371.84	197.02	−77.51
	cc-pVTZ	−183.798 17	1.1565	1907.75	124.13	−183.925 08	1.1036	2357.52	203.76	−79.63
	cc-pVQZ	−183.810 50	1.1547	1907.98	125.05	−183.938 06	1.1020	2357.62	205.10	−80.04
	aug-cc-pVDZ	−183.764 34	1.1635	1907.91	121.50	−183.887 98	1.1153	2357.07	199.10	−77.58
	aug-cc-pVTZ	−183.799 85	1.1564	1899.89	124.32	−183.927 20	1.1035	2353.26	204.22	−79.91
	aug-cc-pVQZ	−183.811 07	1.1547	1907.31	124.87	−183.938 76	1.1020	2352.19	205.35	−80.12
CASPT2(10,9) std	cc-pVDZ	−184.052 11			130.40	−184.157 19			196.36	−65.94
	cc-pVTZ	−184.204 77			140.02	−184.314 44			208.83	−68.82
	cc-pVQZ	−184.255 41			144.22	−184.366 93			214.18	−69.98
	aug-cc-pVDZ	−184.085 51			131.77	−184.188 86			196.61	−64.85
	aug-cc-pVTZ	−184.216 45			140.97	−184.326 07			209.75	−68.78
	aug-cc-pVQZ	−184.260 67			144.83	−184.372 19			214.92	−69.98
CASPT2(10,9) G2	cc-pVDZ	−184.044 25			135.43	−184.152 97			203.67	−68.22
	cc-pVTZ	−184.194 99			146.15	−184.309 44			217.96	−71.82
	cc-pVQZ	−184.244 90			150.79	−184.361 57			224.00	−73.21
	aug-cc-pVDZ	−184.076 09			137.69	−184.184 01			205.40	−67.72
	aug-cc-pVTZ	−184.205 82			147.47	−184.320 75			219.58	−72.12
	aug-cc-pVQZ	−184.249 74			151.61	−184.366 70			225.03	−73.39
CASPT2(10,9) G2[c]	cc-pVTZ	−184.194 99	1.1571	1904.45	146.15	−184.310 22	1.1040	2331.25	218.46	−72.31
CCSD(T)[d]	cc-pVDZ	−184.076 94			131.97	−184.186 31			200.60	−68.63
	cc-pVTZ	−184.231 63			143.57	−184.347 77			216.44	−72.88
	cc-pVQZ	−184.279 26			148.48	−184.397 81			222.87	−74.39
	aug-cc-pVDZ	−184.112 27			133.68	−184.220 81			201.80	−68.11
	aug-cc-pVTZ	−184.243 16			144.91	−184.359 66			218.01	−73.10
MR-CI + Q[e]	cc-pVDZ	−183.885 54			137.21	−183.997 59			207.52	−70.31
	cc-pVTZ	−183.971 09			149.34	−184.092 20			225.32	−75.99
	cc-pVQZ	−183.997 13			154.18	−184.121 29			232.08	−77.91
	aug-cc-pVDZ	−183.905 48			139.42	−184.017 22			209.52	−70.12
	aug-cc-pVTZ	−183.976 51			149.87	−184.098 08			226.15	−76.28
Experimental[f]			1.1508	1904.20	152.53		1.0977	2358.57	228.41	−75.88

[a]CASPT2, energies at the CASSCF optimal geometries with the same basis set and active space.

[b]Reaction exoergicity for $N(^4S)+NO \rightarrow O(^3P)+N_2$.

[c]CASPT2 G2 energies and harmonic vibrational frequencies obtained with the optimal geometries at the same level by using the VIBROT module of the MOLCAS 4.1 program (Ref. 25). Masses of the most abundant isotopes were used: ^{14}N and ^{16}O.

[d]Coupled cluster energies with perturbative contribution at triple excitations (Ref. 32) using initial restricted open shell Hartree–Fock MOs. Energies were calculated at the optimal CASSCF(10,9) geometries.

[e]Multireference configuration interaction energies including the Davidson correction for quadruple excitations (Ref. 31). The N and O 2s electrons were not correlated. Energies were calculated at the optimum CASSCF(10,9) geometries.

[f]The lowest spin-orbit states [i.e., $NO(X\,^2\Pi_{1/2})$ and $O(^3P_2)$] were used for the experimental data (Ref. 34).

TABLE II. *Ab initio* properties of the $^3A''$ transition state (TS1) for the reaction channel (1).[a]

Method	Basis set	E/a.u.	$R_{e(\mathrm{NN})}$/Å	$R_{e(\mathrm{NO})}$/Å	< NNO/°	ω_i/cm^{-1} [b]	ΔE/kcal mol^{-1} [c]
CASSCF(16,12)	cc-pVDZ	−183.753 29	1.7896	1.1719	108.9	417.56 1854.43 241.48i	6.59 (7.10)
	cc-pVTZ	−183.798 23	1.8880	1.1606	109.0	419.70 1794.58 272.17i	5.51 (5.97)
	cc-pVQZ	−183.811 23	1.9103	1.1598	109.2	421.21 1743.24 281.19i	5.32 (5.70)
	aug-cc-pVDZ	−183.764 59	1.8933	1.1676	108.8	418.23 1823.23 262.23i	5.44 (5.94)
	aug-cc-pVTZ	−183.800 61	1.9219	1.1588	109.1	403.38 1803.22 268.29i	5.11 (5.56)
CASPT2(16,12) G2	cc-pVDZ	−184.055 36					−1.76
	cc-pVTZ	−184.240 33					−4.74
	cc-pVQZ	−184.268 32					−5.38
	aug-cc-pVDZ	−184.091 03					−3.83
	aug-cc-pVTZ	−184.258 32					−6.60
CASSCF(10,9)	cc-pVDZ	−183.740 72	1.7287	1.1743	108.76	499.15 1735.87 310.29i	8.83 (9.27)
	cc-pVTZ	−183.786 39	1.8262	1.1610	108.90	455.13 1782.64 285.74i	7.39 (7.86)
	cc-pVQZ	−183.799 15	1.8455	1.1577	109.01	450.83 1792.68 285.95i	7.12 (7.60)
	aug-cc-pVDZ	−183.752 69	1.8368	1.1677	108.68	452.19 1785.80 295.12i	7.31 (7.78)
	aug-cc-pVTZ	−183.788 98	1.8603	1.1585	109.03	443.29 1792.73 280.12i	6.82 (7.30)
CASPT2(10,9) std	cc-pVDZ	−184.052 00					0.07
	cc-pVTZ	−184.209 35					−2.87
	cc-pVQZ	−184.261 93					−4.09
	aug-cc-pVDZ	−184.088 72					−2.01
	aug-cc-pVTZ	−184.223 18					−4.22
CASPT2(10,9) G2	cc-pVDZ	−184.047 27					−1.90
	cc-pVTZ	−184.202 77					−4.88
	cc-pVQZ	−184.254 65					−6.12
	aug-cc-pVDZ	−184.082 15					−3.80
	aug-cc-pVTZ	−184.215 61					−6.14
CCSD(T)[d]	cc-pVDZ	−184.074 49					1.54
	cc-pVTZ	−184.234 75					−1.96
	aug-cc-pVDZ	−184.113 23					−0.60
	aug-cc-pVTZ	−184.248 23					−3.18
MR-CI+Q[e]	cc-pVDZ	−183.886 57					−0.64
	cc-pVTZ	−183.975 53					−2.79
	aug-cc-pVDZ	−183.908 61					−1.97
	aug-cc-pVTZ	−183.982 14					−3.62
CASSCF(10,9)[f]	Duijneveldt [11s6p3d4f/5s3p2d1f]	⋯	1.8193	1.1626	108.5	396 1720 250i	5.0(5.4)
MR-CCI+Q[f]	Duijneveldt [11s6p3d4f/5s3p2d1f]	− ⋯	2.1707	1.1494	108.9	385 1785 210i	0.5(1.0)

[a]CASPT2 energies at the CASSCF optimal geometries with the same basis set.

[b]Harmonic vibrational frequencies: ω_1 (NNO bend., a'), ω_2 (NO str., a') and ω_3 (NN str., a'), respectively. Masses of the most abundant isotopes were used: ^{14}N and ^{16}O.

[c]Energy barrier respect to N(^4S)+NO. The value corrected with the difference of zero point energies is shown in parentheses.

[d]Coupled cluster energies with perturbative contribution at triple excitations (Ref. 32) using initial restricted open shell Hartree–Fock MOs. Energies were calculated at the optimal CASSCF(10,9) geometries.

[e]Multireference configuration interaction energies including the Davidson correction for quadruple excitations (Ref. 31) using 9 CSFs as reference wavefunction. The N and O 2s electrons were not correlated. Energies were calculated at the optimal CASSCF(10,9) geometries.

[f]Previous *ab initio* results from Ref. 15, where the N and O 2s electrons were not correlated in the MR-CCI calculations.

(Refs. 24, 38, 39), N(^2D)+NO (Ref. 40) or N(^2D)+O$_2$ (Refs. 41–44) reactions. Three stationary points were obtained at the CASPT2 level: TS2, MIN1, and TS2′ (Fig. 1). The MEP presents only a C_{2v}-symmetry transition state at CASSCF level with a very high-energy barrier (65.70 kcal/mol). The inclusion of the dynamical correlation energy decreased this barrier to 41.13 kcal/mol and led to a C_s-symmetry transition state (Table III). The TS2 optimal geometry at the CASPT2 level was derived by means of a local fit of 90 points with a final root-mean-square deviation (RMSD) of 0.11 kcal/mol. 240 points were used for the MIN1 characterization with a RMSD of 0.24 kcal/mol. In spite of MIN1 is a very shallow minimum on the lowest $^3A''$ NNO PES, this kind of C_{2v}-minimum is similar to the ones

observed in the lowest $^1A'$ NNO PES (Ref. 40) and in the lowest $^2A'$ and $^4A'$ NOO PESs.[39] A similar structure as that for the peroxy isomer of NO$_2$, with a shallow minimum over reactants or products, reported in early theoretical studies,[45,46] has been later confirmed in more accurate *ab initio* studies,[47] not only for the ground $^2A'$ PES but also for the first excited $^4A'$ PES.[24,39] Although more *ab initio* calculations could be made to characterize even better this minimum and both transitions states, we believe that the main conclusion that reaction channel (2) will be only important on the $^3A''$ PES for collision energies over 41 kcal/mol can be reliably established, in agreement with experimental data, which show only a small contribution of this reaction channel even at high collision energies.[22,23]

J. Chem. Phys., Vol. 118, No. 23, 15 June 2003

N+NO reaction   10607
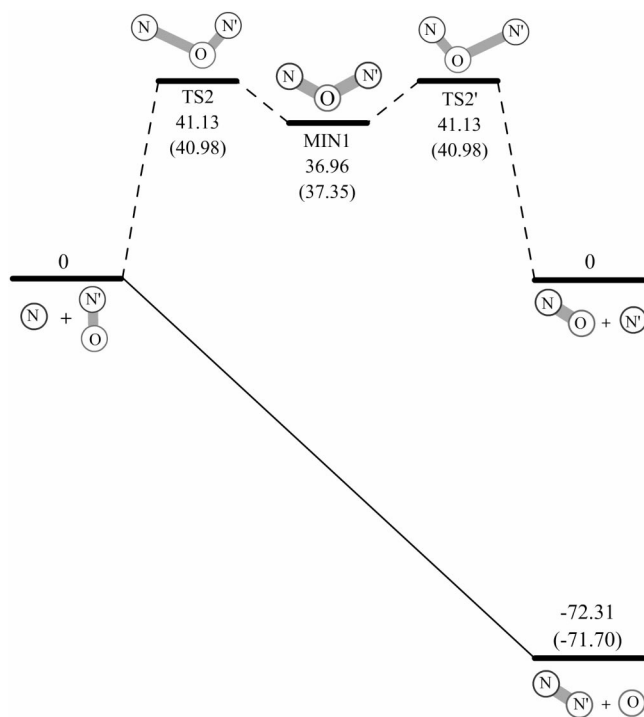
FIG. 1. Energetics of the minimum energy paths for both $N(^4S)+N'O$ reaction channels computed on the lowest $^3A''$ potential energy surface at the CASPT2(10, 9) G2/cc-pVTZ level. The solid line corresponds to the minimum energy pathway for the N abstraction and the dashed lines for the O abstraction. The energies are given in kcal/mol relative to reactants. Energies with the inclusion of zero point energy contributions are given between parentheses.

C. Characterization of the lowest $^3A'$ potential energy surface

Table IV summarizes the properties of the transition state (TS1) found on the $^3A'$ PES for reaction channel (1). It has a similar geometry as TS1 on the $^3A'$ PES. However, in the case of the $^3A'$ PES, this TS is obtained at both the CASSCF and the CASPT2 levels. The present CASSCF properties are close to previously published CASSCF data[15] (Table IV). The full-valence active space CASSCF calculations enlarge 0.1 Å the NN distance. Moreover, the optimization of the geometry at the CASPT2(10,9) level increases significantly (about 0.2 Å) the NN distance with respect to the CASSCF(10,9) calculations. Because of this, the CASPT2 energies derived using the optimal CASSCF geometries are not accurate enough to evaluate the energy barrier

associated to TS1. Although the dynamical correlation reduces considerably the energy barrier, the inclusion of the CASPT2 geometry optimization taking into account a grid of 216 points (with a RMSD=0.063 kcal/mol for the local fit) tend to compensate partially with a small increase of the energy barrier.

A detailed study of the energy barrier of TS1 has been made by increasing the quality of the basis set at the optimal CASPT2(10,9) G2 geometry. The basis set dependence is usually well described by a simple exponential-like function[48] of the form,

$$\Delta E_n^{\neq} = \Delta E_\infty^{\neq} + Be^{-Cn}, \tag{3}$$

where n is the cardinal number of the standard correlation-consistent cc-pVnZ basis set (2, 3, 4, and 5 for DZ, TZ, QZ, and 5Z, respectively) and $\Delta E_\infty^{\neq}$ corresponds to the estimated complete basis set (CBS) limit as $n \to \infty$. The estimated CASPT2(10,9) CBS limit for this energy barrier was equal to 6.74 kcal/mol (B=22.06 kcal/mol, C=0.8702, and r^2=0.99995). This energy barrier is much lower than the previous MR-CCI+Q value[15] (14.4 kcal/mol). This difference is essentially not originated by the *ab initio* method and basis set but by the N and O $2s$ electron correlation contribution than is much more important in the $^3A'$ PES than in the barrierless $^3A''$ PES. This point has been checked by comparing the present MR-CI+Q calculations with the MR-CCI+Q ones,[15] keeping also the atomic $2s$ electrons frozen. The MR-CI+Q calculations were made at the CASSCF(10,9) optimal geometries using the following 9 reference CSFs, where the electronic occupation of the $6a'$ and $3a''$ MOs are indicated: (221100 211), (201120 211), (211110 112), (111111 211), (121101 112), (021102 211), (101121 112), (211110 211), and (201120 112) with a total weight of 0.9982. This originated the following number of CSFs depending on the basis set: 319740 (cc-pVDZ), 2230734 (cc-pVTZ), 8669349 (cc-pVQZ), 1181526 (aug-cc-pVDZ), and 5864184 (aug-cc-pVTZ) to be compared with the previous MR-CCI calculations[15] with approximately 1 000 000 of CSFs. Similar energy barriers were found in both cases (Table IV). If CASPT2 optimal geometries were used instead of the CASSCF ones a closer agreement could be expected.

CASPT2 calculations correlated also the N and O $2s$ electrons. Thus, for example, the CASPT2(10,9) G2 energy for cc-pVDZ, cc-pVTZ, and cc-pVQZ basis sets at the cor-

TABLE III. *Ab initio* properties of the $^3A''$ stationary points for the exchange reaction channel (N+ON') with the (10,9) active space and the cc-pVTZ basis set.

Stationary point	Method	E/a.u.	$R_{e(NO)}$/Å	$R_{e(ON')}$/Å	<NON'/°	ω_i/cm^{-1} [a]	ΔE/kcal mol^{-1} [b]
TS2	CASSCF	−183.693 47	1.3292	1.3292	102.07	300.07 1300.85 385.25i	65.70 (65.26)
	CASPT2 G2[c]	−184.129 44	1.4597	1.2294	100.59	424.92 1372.63 249.50i	41.13 (40.98)
MIN1	CASSCF						not present
	CASPT2 G2	−184.136 09	1.3238	1.3238	104.84	672.25 1276.23 225.61	36.96 (37.35)

[a]Harmonic vibrational frequencies: (a) $C_s : \omega_1$ (NON' bend., a'), ω_2 (ON' str., a'), ω_3 (NO str., a'), respectively, and (b) $C_{2v} : \omega_1$ (NON' bend., a_1), ω_2 (sym. str., a_1), ω_3 (asym. str., b_2), respectively (YZ taken as the molecular plane). Masses of the most abundant isotopes were used: ^{14}N and ^{16}O.
[b]Energy respect to $N(^4S)+ON'$. The value corrected with the difference of zero point energies is shown in parentheses.
[c]There are two equivalent transition states (TS2 and TS2') exchanging both NO distances.

TABLE IV. *Ab initio* properties of the $^3A'$ transition state (TS1) for the reaction channel (1).[a]

Method	Basis set	E/a.u.	$R_{e(\text{NN})}$/Å	$R_{e(\text{NO})}$/Å	$<\text{NNO}$/°	ω_i/ cm^{-1} [b]	ΔE/ kcal mol^{-1} [c]
CASSCF(16,12)	cc-pVDZ	−183.728 96	1.8101	1.1732	117.41	377.08 1796.53 761.62i	21.91 (22.28)
	cc-pVTZ	−183.773 22	1.8252	1.1663	117.43	380.02 1733.24 771.01i	21.26 (21.57)
	cc-pVQZ	−183.785 65	1.8267	1.1638	117.55	378.89 1735.62 769.37i	21.19 (21.50)
	aug-cc-pVDZ	−183.739 07	1.8230	1.1734	117.42	379.10 1784.13 752.23i	21.50 (21.88)
	aug-cc-pVTZ	−183.775 31	1.8283	1.1653	117.55	380.24 1732.65 773.86i	20.98 (21.30)
CASPT2(16,12) G2	cc-pVDZ	−184.052 28					2.03
	cc-pVTZ	−184.224 89					4.94
	cc-pVQZ	−184.326 98					3.63
	aug-cc-pVDZ	−184.075 31					5.65
	aug-cc-pVTZ	−184.243 75					2.54
CASSCF(10,9)	cc-pVDZ	−183.706 48	1.7315	1.1779	115.73	433.17 1660.97 873.27i	30.31 (30.55)
	cc-pVTZ	−183.751 44	1.7438	1.1703	115.87	425.58 1660.95 858.10i	29.32 (29.58)
	cc-pVQZ	−183.763 96	1.7454	1.1677	115.89	425.33 1665.18 855.94i	29.20 (29.46)
	aug-cc-pVDZ	−183.717 22	1.7433	1.1777	115.73	420.99 1655.18 854.00i	29.57 (29.81)
	aug-cc-pVTZ	−183.753 70	1.7463	1.1692	115.93	423.62 1656.70 849.19i	28.96 (29.22)
CASPT2(10,9) std	cc-pVDZ	−184.037 18					9.37
	cc-pVTZ	−184.196 68					5.08
	cc-pVQZ	−184.249 97					3.41
	aug-cc-pVDZ	−184.075 14					6.51
	aug-cc-pVTZ	−184.212 04					2.77
CASPT2(10,9) G2	cc-pVDZ	−184.035 07					5.76
	cc-pVTZ	−184.192 89					1.32
	cc-pVQZ	−184.245 51					−0.38
	aug-cc-pVDZ	−184.071 28					3.02
	aug-cc-pVTZ	−184.206 49					−0.42
CASPT2(10,9) G2	cc-pVTZ	−184.181 68	1.9680	1.1578	116.04	251.89 1820.48 450.23i	8.38 (8.59)
CASPT2(10,9) std.	cc-pVTZ	−184.196 48	1.9367	1.1621	116.08	290.28 1920.23 434.78i	5.20 (5.64)
CCSD(T)[d]	cc-pVDZ	−184.051 94					15.67
	cc-pVTZ	−184.213 02					11.68
	aug-cc-pVDZ	−184.092 04					12.70
MR-CI + Q[e]	cc-pVDZ	−183.859 40					16.40
	cc-pVTZ	−183.950 20					13.11
	cc-pVQZ	−183.976 73					12.80
	aug-cc-pVDZ	−183.883 86					13.56
	aug-cc-pVTZ	−183.957 86					11.70
CASSCF(10,9)[f]	Duijneveldt $[11s6p3d4f/5s3p2d1f]$	⋯	1.7590	1.1906	116.5	383 1586 727i	25.3 (25.5)
MR-CCI+Q[f]	Duijneveldt $[11s6p3d4f/5s3p2d1f]$	⋯	1.8913	1.1695	116.5	383 1678 569i	14.4 (14.71)

[a]CASPT2 energies at the CASSCF optimal geometries with the same basis set.

[b]Harmonic vibration frequencies: ω_1 (NNO bend., a'), ω_2 (NO str., a'), and ω_3 (NN str., a'), respectively. Masses of the most abundant isotopes were used: ^{14}N and ^{16}O.

[c]Energy barrier with respect to N(^4S) + NO. The value corrected with the difference of zero point energies is shown in parentheses.

[d]Coupled cluster energies with perturbative contribution at triple excitations (Ref. 32) using initial restricted open shell Hartree–Fock MOs. Energies were calculated at the optimal CASSCF(10,9) geometries.

[e]Multireference configuration interaction energies including Davidson correction for quadruple excitations (Ref. 31) using 9 CSFs as a reference wavefunction. The N and O 2s electron were not correlated. Energies were calculated at the optimal CASSCF(10,9) geometries.

[f]Previous *ab initio* results from Ref. 15, where the N and O 2s electrons were not correlated in the MR-CCI calculations.

responding CASSCF optimal geometry (5.76, 1.32, and −0.38 kcal /mol, respectively; see Table IV) become much more larger when 2s electron correlation is neglected (i.e., 19.45, 14.34, and 13.17 kcal/mol, respectively), leading to values close to the MR-CCI+Q ones. Therefore, seems to be clear that the N and O 2s electrons need to be correlated to produce reliable energies in the $^3A'$ PES.

In a similar way as for the lowest $^3A''$ PES, we have studied the reaction channel (2) by using the CASSCF(10,9) and the CASPT2 (10,9) G2 methods and the cc-pVTZ basis set. Figure 2 gives the MEP found for this PES, considering reactions channels (1) and (2). Three stationary points were also obtained for the second reaction channel at the CASPT2 level, which were very analogous to those of the $^3A''$ PES.
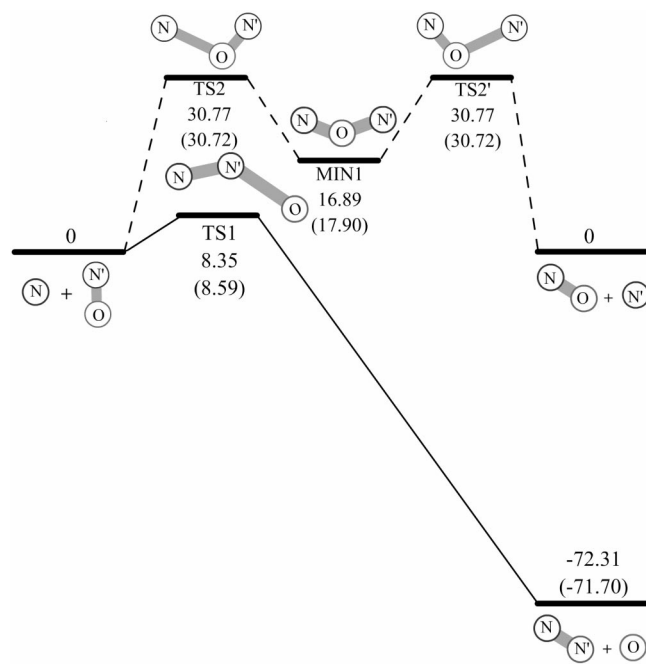
FIG. 2. Energetics of the minimum energy paths for both $N(^4S)+N'O$ reaction channels computed on the lowest $^3A'$ potential energy surface at the CASPT2(10, 9) G2/cc-pVTZ level. The solid line corresponds to the minimum energy pathway for the N abstraction and the dashed lines for the O abstraction. The energies are given in kcal/mol relative to reactants. Energies with the inclusion of zero point energy contributions are given between parentheses.

Table V summarizes the properties of these stationary points. The CASSCF and CASPT2 methods agree with each other showing a C_s-symmetry transition state (TS2). The high-energy barrier (57.11 kcal/mol) at the CASSCF(10,9) level becomes smaller when the CASPT2(10,9) G2 method is considered (30.77 kcal/mol). There was also found a C_{2v}-minimum (MIN1) between both equivalent transition states (i.e., TS2 and TS2'). The CASPT2 TS2 optimal geometry was obtained by means of a local fit of 756 points with a final RMSD of 0.0002 kcal/mol. 660 points were used for the MIN1 characterization with a RMSD of 0.0016 kcal/mol. One important conclusion that can be derived from these results is that for collision energies over 30 kcal/mol the second reaction channel will be open through the $^3A'$ PES, becoming even more accessible than through the $^3A''$ PES. Our recent quasiclassical trajectory study using the lowest $^1A'$ PES (Ref. 40) on the $N(^2D)+NO(X\,^2\Pi)$ reactions gives

a rate constant branching ratio [i.e., $k_2/(k_1+k_2)$ but with $N(^2D)$ instead of $N(^4S)$] of 3.02% for the equivalent O-abstraction reaction channel at 1500 K, although this PES presents a MEP with the stable $NNO(X\,^1\Sigma^+)$ minimum (ground state of the NNO molecule) and without almost an effective energy barrier (there are several MEPs for this reaction[40]). Thus, experimental studies should be required to corroborate the real contribution of this O-abstraction reaction channel (i.e., N-exchange reaction channel) to the total reactivity at high collision energies (or temperatures) for atomic nitrogen in its lowest electronic states (i.e., ^4S, ^2D, and ^2P).

IV. CONCLUSIONS AND REMARKS

This work presents a theoretical study of the two $N(^4S)+NO(X\,^2\Pi)$ abstraction reaction channels on the lowest $^3A''$ and $^3A'$ potential energy surfaces. *Ab initio* CASSCF, CASPT2, CCSD, and MR-CI methods with standard correlation-consistent (cc-pVnZ and aug-cc-pVnZ, $n=$D, T, Q, 5) Dunning's basis sets were used. Moreover, the complete basis set limit extrapolated result was also reported for the energy barrier of reaction channel (1) on the $^3A'$ PES.

The ground $^3A''$ PES does not have an energy barrier along the MEP for the most important reaction channel (1), and shows a very high-energy barrier (TS2) for reaction channel (2). The $^3A'$ PES presents an energy barrier (TS1) of 6.74 kcal/mol for reaction channel (1), a value that is much lower than the previously published results (i.e., 14.4 kcal/mol at MR-CCI+Q/[$11s6p3d4f/5s3p2d1f$]) (Ref. 15). The present analysis of the influence of the N and O $2s$ electron correlation in the MR-CI and CASPT2 results shows that it is very important to correlate the $2s$ electrons, in both type of calculations (CASPT2 and MR-CI). This produces lower energy barriers, also in agreement with our recent theoretical studies on the analogous $N(^4S)+O_2$ reaction.[24] This point was not taken into account in previous *ab initio* studies.

The $^3A'$ PES shows also a high-energy barrier (30.77 kcal/mol) for reaction channel (2) but smaller than the one found in the $^3A''$ PES (41.13 kcal/mol). Although the reaction channel (1) will be only accessible through the $^3A''$ PES at room temperature, the second PES will become also relevant at higher temperatures. Moreover, reaction channel (2) will be only open at high temperatures (e.g., collision energies over 30 kcal/mol). Experimental studies would be of interest to confirm the real contribution of this O-abstraction

TABLE V. *Ab initio* properties of the $^3A'$ stationary points for the exchange reaction channel $(N+ON')$ with the (10,9) active space and the cc-pVTZ basis set.

Stationary point	Method	E/a.u.	$R_{e(NO)}$/Å	$R_{e(ON')}$/Å	$<$ NON'/°	ω_i/ cm^{-1} [a]	ΔE/kcal mol^{-1} [b]
TS2[c]	CASSCF	-183.70715	1.6042	1.2180	120.07	478.05 1184.43 1114.35i	57.11 (56.76)
	CASPT2 G2	$-184.145\,95$	1.7104	1.1836	123.12	419.81 1448.40 958.02i	30.77 (30.72)
MIN1	CASSCF	$-183.723\,41$	1.3160	1.3160	120.34	536.10 1038.57 962.56	43.81 (44.71)
	CASPT2 G2	$-184.168\,07$	1.3001	1.3001	124.20	522.92 1066.31 1021.27	16.89 (17.90)

[a]Harmonic vibrational frequencies: (a) C_s: ω_1 (NON' bend., a'), ω_2 (ON' str., a'), ω_3 (NO str., a'), respectively, and (b) C_{2v}: ω_1 (NON' bend., a_1), ω_2 (sym. str., a_1), ω_3 (asym. str., b_2), respectively (YZ taken as the molecular plane). Masses of the most abundant isotopes were used: ^{14}N and ^{16}O.
[b]Energy respect to $N(^4S)+ON'$. The value corrected with the difference of zero point energies is shown in parentheses.
[c]There are two equivalent transition states (TS2 and TS2') exchanging both NO distances.

reaction channel to the total reactivity at high temperatures.

The present results significantly improve previous high quality *ab initio* studies and, in particular, provide a much lower energy barrier for the $^3A'$ PES, which will produce larger values of the thermal rate constants at high temperatures. On the other hand, two analytical PESs ($^3A''$ and $^3A'$) based on several grids of *ab initio* points are currently in progress in our group and will be used in kinetics and dynamics studies on this reaction.

ACKNOWLEDGMENTS

[1] M. W. Chase, Jr., C. A. Davies, J. R. Downey, Jr., D. J. Frurip, R. A. McDonald, and A. N. Syverud, J. Phys. Chem. Ref. Data Suppl. **14**, 1 (1985).

[2] D. E. Siskind and D. W. Rusch, J. Geophys. Res. **97**, 3209 (1992).

[3] P. O. Wennberg, J. G. Anderson, and D. K. Weisenstein, J. Geophys. Res. **99**, 18839 (1994).

[4] P. Warneck, in *Chemistry of the Natural Atmosphere* (Academic, San Diego, 1998), Chap. 3.

[5] G. Marston, Chem. Soc. Rev. **25**, 33 (1996).

[6] T. Kurotaki, AIAA paper No. 2000-2366, 2000.

[7] D. L. Baulch, C. J. Cobos, R. A. Cox *et al.*, J. Phys. Chem. Ref. Data **23**, 847 (1994).

[8] W. B. DeMore, D. M. Golden, R. F. Hampson, M. J. Kurylo, C. J. Howard, A. R. Ravishankara, C. E. Kolb, and M. J. Molina, in *Chemical Kinetics and Photochemical Data for Use in Stratospheric Modeling*, in Evaluation 12, JPL Publ. 97-4 (Jet Propulsion Laboratory, Pasadena, California, 1997).

[9] J. L. Fox, J. Geophys. Res. **99**, 6273 (1994).

[10] J. L. Fox, J. Geophys. Res. **101**, 7987 (1996).

[11] G. Black, R. L. Sharpless, and T. G. Slanger, J. Chem. Phys. **58**, 4792 (1973).

[12] J. E. Morgan and H. I. Schiff, Can. J. Chem. **41**, 903 (1963).

[13] J. E. Morgan, L. F. Phillips, and H. I. Schiff, Discuss. Faraday Soc. **33**, 118 (1962).

[14] M. Gilibert, A. Aguilar, M. González, F. Mota, and R. Sayós, J. Chem. Phys. **97**, 5542 (1992).

[15] S. P. Walch and R. L. Jaffe, J. Chem. Phys. **86**, 6946 (1987); AIP Document No. PAPSJCPSA-86-6946-10.

[16] M. Gilibert, A. Aguilar, M. González, and R. Sayós, J. Chem. Phys. **99**, 1719 (1993).

[17] A. Aguilar, M. Gilibert, X. Giménez, M. González, and R. Sayós, J. Chem. Phys. **103**, 4496 (1995).

[18] R. Sayós, A. Aguilar, M. Gilibert, and M. González, J. Chem. Soc., Faraday Trans. **89**, 3223 (1993).

[19] J. W. Duff and R. D. Sharma, Geophys. Res. Lett. **32**, 2777 (1996).

[20] J. W. Duff and R. D. Sharma, Chem. Phys. Lett. **265**, 404 (1997).

[21] D. Bose and G. V. Candler, J. Chem. Phys. **104**, 2825 (1996).

[22] J. Dubrin, C. Mackay, and R. Wolfgang, J. Chem. Phys. **44**, 2208 (1966).

[23] R. Iwata, A. Ferrieri, and A. P. Wolf, J. Phys. Chem. **90**, 6722 (1986).

[24] R. Sayós, C. Oliva, and M. González, J. Chem. Phys. **115**, 1287 (2001).

[25] MOLCAS 4.1, K. Andersson, M. R. A. Blomberg, M. P. Fülscher *et al.* (Lund University, Sweden, 1998).

[26] B. O. Roos, P. R. Taylor, and P. E. M. Siegbahn, Chem. Phys. **48**, 157 (1980).

[27] B. O. Roos, in *Advances in Chemical Physics: Ab Initio Methods in Quantum Chemistry-II*, edited by K.P. Lawley (Wiley, Chichester, 1987), Vol. LXIX, p. 399.

[28] K. Andersson, Theor. Chim. Acta **91**, 31 (1995).

[29] E02 and E04 subroutines from the NAG Fortran Library Mark 15. The Numerical Algorithms Group Ltd., Oxford, UK.

[30] W. C. Ermler, H. C. Hsieh, and L. B. Harding, Comput. Phys. Commun. **51**, 257 (1988).

[31] E. R. Davidson and D. W. Silver, Chem. Phys. Lett. **53**, 403 (1977).

[32] J. D. Watts, J. Gauss, and R. J. Barlett, J. Chem. Phys. **98**, 8718 (1983).

[33] T. H. Dunning, Jr., J. Chem. Phys. **90**, 1007 (1989).

[34] K. P. Huber and G. Herzberg, *Molecular Spectra and Molecular Structure. Vol. IV. Constants of Diatomic Molecules* (Van Nostrand Reinhold, New York, 1979).

[35] J. Almlöf and P. R. Taylor, J. Chem. Phys. **86**, 4070 (1987).

[36] K. A. Peterson, R. A. Kendall, and T. H. Dunning, Jr., J. Chem. Phys. **99**, 9790 (1993).

[37] K. A. Peterson, A. K. Wilson, D. E. Woon, and T. H. Dunning, Jr., Theor. Chem. Acc. **97**, 251 (1997).

[38] R. Sayós, C. Oliva, and M. González, J. Chem. Phys. **117**, 670 (2002).

[39] M. González, C. Oliva, and R. Sayós, J. Chem. Phys. **117**, 680 (2002).

[40] M. González, R. Valero, and R. Sayós, J. Chem. Phys. **113**, 10983 (2000).

[41] M. González, I. Miquel, and R. Sayós, Chem. Phys. Lett. **335**, 339 (2001).

[42] M. González, I. Miquel, and R. Sayós, J. Chem. Phys. **115**, 2530 (2001).

[43] M. González, I. Miquel, and R. Sayós, J. Chem. Phys. **115**, 8838 (2001).

[44] M. González, I. Miquel, and R. Sayós, Chem. Phys. Lett. **360**, 521 (2002).

[45] H. F. Schaefer III, C. F. Bender, and J. H. Richardson, J. Phys. Chem. **80**, 2035 (1976).

[46] C. Meredith, R. D. Davy, G. E. Quelch, and H. F. Schaefer III, J. Chem. Phys. **94**, 1317 (1991).

[47] S. P. Walch, J. Chem. Phys. **102**, 4189 (1995).

[48] K. A. Anderson and T. H. Dunning, Jr., J. Phys. Chem. A **101**, 6280 (1997).